Generation of photocurrent in quantum dot infrared photodetectors: Role of Pauli correlations

V. M. Apalkov
Department of Physics and Astronomy, Georgia State University, Atlanta, Georgia 30303, USA
(Received 10 July 2006; revised manuscript received 30 November 2006; published 30 January 2007)

We report on our study of the role of the Pauli exclusion principle in the generation of photocurrent in quantum dot infrared photodetectors. The properties of photodetectors are determined by the balance between relaxation and photogeneration rates. Due to the Pauli principle, the relaxation rate depends on the number of available states in the quantum dots. This dependence is strong for small quantum dots with few levels in each dot and weak for large quantum dots or quantum wells. We study both the *I-V* characteristics of the system and low-frequency current noise. In *I-V* dependence, the Pauli principle enhances the photocurrent at a given bias voltage. The current noise has more complicated dependence. At low bias voltage, the Pauli principle enhances the noise, while at high voltage, the exclusion principle suppresses the noise of the current. With increasing intensity of illumination, the effects of the Pauli principle are suppressed due to depletion of the dot levels.

DOI: 10.1103/PhysRevB.75.035339 PACS number(s): 73.21.La, 73.50.Pz, 85.30.−z, 72.70.+m

I. INTRODUCTION

Infrared photodetectors (IPs) based on the nanostructures have been the subject of intensive research during the past decades.[1] The active regions of such photodetectors consist of quantum wells,[1] quantum dots,[2,3] or their combinations.[4] Without illumination and at low temperature, the electrons are in the ground state of the IP system and are bound to its active regions. Under an external illumination, the electrons are excited into weakly bound or continuum states of IPs. Application of the bias voltage to the system results in the photocurrent. Depending on the structure of IP, the optical transitions within the active region of IP can be either bound to bound or bound to continuum. To generate the photocurrent in the case of bound to bound transitions, the electron in the excited bound state should finally tunnel or be thermally excited into the continuum states. Below, we discuss only IP with transitions of bound to continuum type. The properties of such IPs are determined by two basic processes: (i) absorption of a photon by bound electron within the active region of IP and (ii) relaxation transitions of electrons from continuum states into the bound states. Competition between these two processes determines the electron population of the continuum states and consequently the photocurrent and noise in such structures. The main difference between quantum well and quantum dot IPs is in the nature of bound state.[5] In quantum well infrared photodetectors (QWIPs), the electron system in the ground state is a two-dimensional one. The motion of electrons in the z direction (growth direction) is quantized, while in the (x,y) plane the energy spectrum is continuous. In quantum dot infrared photodetectors (QDIPs), the electronic dot system is zero dimensional and the electron motion is quantized in both z and (x,y) directions. Due to the discrete nature of the energy spectra of quantum dots, the Fermi statistics of electrons and Coulomb interactions between them become especially important when different processes related to the transport through the system are studied. In the case of resonant tunneling transport through the dot system, the Fermi statistics results, for example, in sub-Poissonian short noise,[6] while the interelectron interactions produce the Coulomb blockade.[7] Advantages of quantum dot over quantum well infrared photodetectors have been discussed in the literature within the single-electron picture.[2,5] They are related to the modification of relaxation and photoexcitation rates in quantum dot structures compared to quantum well one.

In the present paper, we study the role of electron correlations in the generation of photocurrent in QDIP. Specifically, we concentrate on the Pauli exclusion principle for electrons; i.e., each level can be occupied only by a single electron. We compare the results for QDIP containing quantum dots of large size to the results for QDIP containing quantum dots of small size. In the first case, QDIP has many bound states and the effect of the Pauli principle becomes suppressed. With increasing the size of the dots, the system is finally transformed into QWIP. For small enough quantum dots, there is only one level per dot. In this case, the exclusion statistics becomes crucial, which was already mentioned in the literature.[6] Below, we assume that by varying the size of the dot we change only the "strength" of the Fermi statistics, but all other parameters, such as relaxation and photogeneration rates, remain the same. These rates can have strong dependence on the geometry of the system, suppressing, for example, the relaxation transitions in the quantum dots due to phonon bottleneck.[8] We will not discuss this dependence and will address only the effects of the Pauli principle on the *I-V* structure and photocurrent noise in QDIP. The thermal effects and the dark current will not be considered in the present paper.

The paper is organized as follows. In Sec. II, we present the model of QDIP. Based on the model, we derive the main system of equations, which describe both stationary and nonstationary processes in QDIP. In the model, we also introduce parameter α, which characterizes the strength of the Pauli exclusion principle. With increasing the size of quantum dots, the parameter α is varied from 1 (for small quantum dots) to 0 (for large quantum dots or quantum wells). In Sec. III, we present the solution of the main system of equations in the stationary regime and study the dependence of *I-V* characteristics and the current noise on the strength of exclusion principle and on the number of quantum dot layers in QDIP. Concluding remarks are presented in Sec. V.

FIG. 1. Quantum dot infrared photodetector is shown schematically for $N=4$ layers of quantum dots and $N+1=5$ barriers. The label (QD) stands for quantum dot layers. The left and right contacts are in quasiequilibrium, which are characterized by chemical potentials μ_L and μ_R, respectively. The dotted lines illustrate the levels of quantum dots.

II. THE MODEL AND THE MAIN SYSTEM OF EQUATIONS

Quantum dot infrared photodetectors consist of N active regions, which are separated by potential barriers.[2] The first and the last active regions are connected to the left (emitter) and to the right (collector) contacts through the potential barriers. Each active region of QDIP contains a two-dimensional array of randomly distributed quantum dots. The QDIP is shown schematically in Fig. 1 for $N=4$ active regions, i.e., quantum dot layers. In terms of continuous and bound states, quantum dot infrared photodetectors contain N domains of bound states (arrays of quantum dots) and $N+1$ domains of continuous states (barriers). The electrons in the bound (ground) states of the active regions can be excited into continuous states due to absorption of photons or due to activation processes. Below, we study only the case of large photon flux, so the main channel for electron transition from bound to continuous states is the photon absorption. Under an external bias voltage, the electrons in the continuous states determine the photocurrent through the system. Generally, the electron current has two contributions: due to diffusion of carrier and due to drift under an external electric field. Under the standard regime of operation of infrared photodetectors, the drift term gives the main contribution to the electric current. Below, we take into account only the drift electrical current.

The system of electrons in the bound states of a single active region of QDIP is characterized by an equilibrium (without illumination and at zero bias voltage) electron areal density N_D, which can be estimated as the number of occupied levels in each quantum dot multiplied by the areal density of quantum dots in a single active layer. In this definition, we assume that electrons are spinless; i.e., each quantum dot level can be occupied by a single electron. The electron spin can be easily taken into account by increasing the electron density by a factor of 2 in all equations below. For small quantum dots with a single bound level and a single electron per dot, the equilibrium density is just a real density of quantum dots. Under illumination of QDIP system and under external bias voltage, the bound states of quantum dots are partially occupied. Then, each active region is characterized by the fraction of levels, f_i $(i=1,\ldots,N)$, which are occupied; i.e., there are $f_i N_D$ electrons in the active region i.

The system of electrons in the continuous states is characterized by the volume electron density n_i and by the values of the electric field E_i where $i=1,\ldots,N+1$. Here, E_1 and E_{N+1} are the values of the electric field at emitter and collector contacts, respectively.

The electron density n_i, electric field E_i in the barrier regions, and electron population of QD layers f_i should be obtained from the solution of continuity equation for electrons in continuum states and balance equation for electrons in the bound states of quantum dots together with the Poisson equation for electric field. The corresponding system of equations can be written as[9,10]

$$\frac{dn_i}{dt} = \mu \frac{n_{i+1}E_{i+1} - n_i E_i}{L_w} + g f_i N_D - s(1-\alpha f_i) n_i N_D + \Delta_i^{(\mathrm{gr})}, \tag{1}$$

$$N_D \frac{df_i}{dt} = s(1-\alpha f_i) n_i N_D - g f_i N_D - \Delta_i^{(\mathrm{gr})}, \tag{2}$$

$$E_{i+1} - E_i = -\frac{e}{\kappa} N_D (1 - f_i), \tag{3}$$

where $i=1,\ldots,N$, μ is the mobility of electrons in the barrier region, e is the absolute value of electron charge, and κ is dielectric constant. The length L_w is the width of quantum dot layer. We assume that this width is the same for all quantum dot layers and it is much smaller than the width of the barriers L_b. The coefficients g and s determine the generation rate (due to absorption of photons) and recombination rate (due to relaxation processes and trapping), respectively. In such definition, g is proportional to the photon flux. Both coefficients g and s depend on the local electric field[11,12] due to redistribution of electric charges around the active region of IP. Such dependence can result in formation of irregular domain structure within IP regions.[13,14] In the present study, we disregard this dependence and assume that both g and s are independent of the local electric field E_i. It is also assumed in Eqs. (1) and (2) that the electric field and electron density are constant within each barrier. In the Poisson equation, Eq. (3), only the electrons in the quantum dot layers but not in the continuum were taken into account.

The numerical coefficient α in Eqs. (1) and (2) characterizes the strength of the Pauli exclusion principle for electrons. For small quantum dots, the coefficient α is equal to 1, while for large quantum dots (quantum well), $\alpha \approx 0$. To study the current noise in QDIP system, we also included in Eqs. (1) and (2) the source of the noise, $\Delta_i^{(\mathrm{gr})}$, which is due to generation-recombination processes. Functions $\Delta_i^{(\mathrm{gr})}(t)$ describe the Poisson processes with zero average and power spectral density $4g\langle f_i\rangle N_D$, where $\langle\cdots\rangle$ stands for the time average.[10,15]

The electric current density in the barrier i is determined by mobility μ of electrons in the continuous states and is given by the expression

$$J_i = \mu n_i E_i. \tag{4}$$

The net current density through the system is expressed in terms of the average current density over all $N+1$ barriers and has the following form:

$$J = \frac{\sum_{i=1}^{N+1} J_i}{N+1} = \frac{\sum_i \mu n_i E_i}{N+1}. \quad (5)$$

The system of equations (1)–(5) determines the bulk properties of QDIP. To describe the interaction of QDIP with the contacts, we need to add the boundary conditions. One boundary condition determines the character of injection of electrons into the QDIP system from emitter contact. The injection of electrons is determined by the properties of the first (emitter) barrier. There are two basic mechanisms of electron injection: (i) tunneling injection[16] and (ii) thermionic injection.[17] At large enough electric field at the emitter contact or at low enough temperature, the tunneling injection gives the main contribution to the electric current. In the present paper, we consider only this type of injection. Under tunneling injection, the electrons are tunneling from the emitter into continuum states and determine the current in the first (emitter) barrier. For the triangular shape of the emitter barrier, the injected current density J_{in} depends on the electric field at the emitter and is given by the expression[16]

$$J_{\text{in}} = J_{\max} \exp(-E_t/E_1), \quad (6)$$

where $J_{\max}$ is the maximum current density, E_t is the characteristic electric field of the emitter barrier, and E_1 is the actual electric field at the emitter. For strong electric field at emitter barrier E_1, both $J_{\max}$ and E_t have weak dependence on the electric field E_1 and are determined only by the parameters of the barrier. For weak enough electric field E_1, the tunneling current becomes strongly suppressed. In this case, the main contribution to the injected electric current becomes thermionic.[17]

Taking into account the fact that injected current is equal to the current in the first barrier, we write the first boundary condition as

$$J_{\text{in}} = J_1 = \mu n_1 E_1. \quad (7)$$

The solution of the system of equations (1)–(7) determines the distribution of electrons and electric field along QDIP for a given value of the net current density J through QDIP. Then, the applied bias voltage V between emitter and collector contacts can be found from the following expression:

$$V = L_b \sum_{i=1}^{N+1} E_i. \quad (8)$$

Equation (8) should be considered as the second boundary condition for the system of equations (1) and (2).

Finally, Eqs. (1)–(7) together with the expression for the bias voltage [Eq. (8)] determine the properties of the system.

III. SOLUTION OF THE MAIN SYSTEM OF EQUATIONS

A. Stationary regime

To find I-V characteristics of QDIP, we need to find the stationary solution of the system of equations (1)–(8). In this case the sources of generation-recombination noise $\Delta_i^{(\text{gr})}$ and the time derivatives in Eqs. (1) and (2) are zero. Substituting Eq. (2) into Eq. (1), we obtain the conservation of the current through the whole region of QDIP:

$$J = \mu n_1 E_1 = \mu n_i E_i, \quad i = 2, \ldots, N+1. \quad (9)$$

In the stationary regime, the balance equation (2) for electrons in the dot layers becomes

$$s(1-\alpha f_i) n_i N_D = g f_i N_D, \quad i = 1, \ldots, N. \quad (10)$$

The boundary condition (6), which determines the injected current into QDIP system, can be written as

$$J = J_{\max} \exp(-E_t/E_1), \quad (11)$$

where the conservation of the current [Eq. (9)] has been taken into account. Equation (11) relates now the total current through the system with the parameters of the emitter barrier.

The solution of the main system of equations in the stationary regime can be found in the following way. From Eqs. (9) and (10), we can express the electron density n_i and the occupation of the quantum dots f_i in terms of the photocurrent density J and the local electric field E_i. Then, we substitute these expressions into Eq. (3) and find the recurrent equation, which relates E_{i+1} and E_i. Taking into account that the electric field in the first (emitter) barrier can be found from Eq. (11), we obtain the closed system of equations describing the distribution of the electric field in QDIP under the fixed value of the current density J. Finally, the solution of the main system of equations can be written as

$$E_1 = E_t/\ln(J_{\max}/J), \quad (12)$$

$$E_{i+1} = E_i - \epsilon \frac{E_i/E_J + \alpha - 1}{E_i/E_J + \alpha}, \quad i = 1, \ldots, N, \quad (13)$$

where the new notations have been introduced:

$$\epsilon = eN_D/\kappa,$$

$$E_J = sJ/(\mu g).$$

The electric field E_J is an effective electric field which would produce the drift current density J if the density of electrons in continuous states is g/s.

From Eqs. (12) and (13), we can find the values of E_i in terms of the current density J. With the known values of E_i, we can express the bias voltage [see Eq. (8)] as a function of current J. This dependence finally gives the I-V characteristics of QDIP.

For a single layer quantum dot infrared photodetector, $N=1$, the system of equations (12) and (13) can be easily solved, resulting in the following I-V dependence:

$$\frac{V}{L_b} = 2E_1 - \epsilon \frac{E_1/E_I + \alpha - 1}{E_1/E_J + \alpha} = 2E_1 - \epsilon + \epsilon \frac{1}{E_1/E_J + \alpha}$$

$$= \frac{2E_t}{\ln(J_{\max}/J)} - \epsilon + \frac{\epsilon E_J \ln(J_{\max}/J)}{E_t + \alpha E_J \ln(J_{\max}/J)}. \quad (14)$$

We can see from this expression that for a given value of

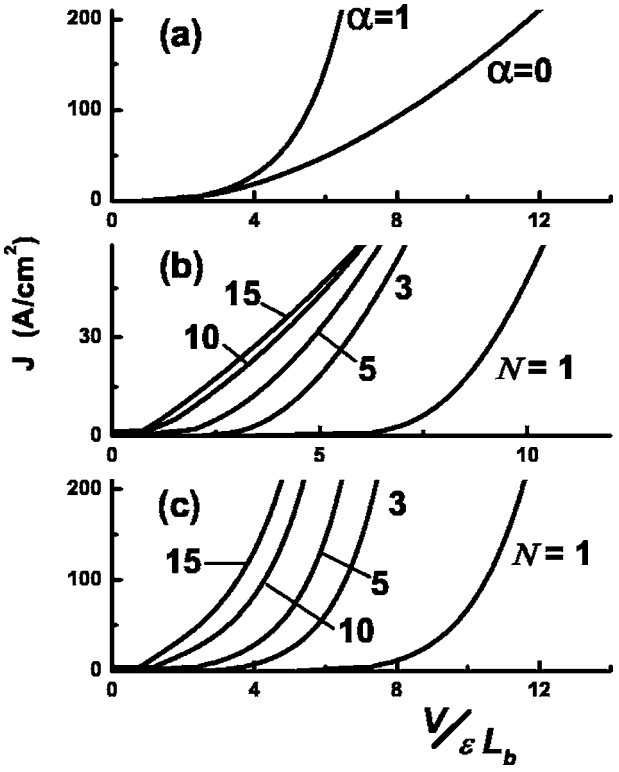

FIG. 2. Photocurrent as a function of bias voltage is shown for different values of parameter α and different numbers of quantum dot layers: (a) QDIP with a single quantum dot layer, $N=1$, $\alpha=1$, and $\alpha=0$; (b) $\alpha=0$ and different N (numbers by the lines are the values of N); and (c) $\alpha=1$ and different N (numbers by the lines are the values of N).

current density J, the increase of parameter α decreases the voltage across QDIP. Therefore, for the same bias voltage the photocurrent through QDIP with small quantum dots ($\alpha=1$) is larger than the photocurrent through QDIP with large quantum dots or through QWIP ($\alpha\approx 0$).

This tendency remains the same for a larger number of quantum dot layers. In Fig. 2, we present the results of the numerical solution of the system (12) and (13) for different numbers of quantum dot layers. To reduce the number of parameters, which determine the properties of the system, we measure the electric field in units of ϵ and the voltage in units of ϵL_b. The photocurrent through the QDIP system can also be presented as a dimensionless quantity if we introduce the ratio $J/J_{\max}$. Since for the typical QDIP structures this ratio can be very large, we will keep below the original units ($\mathrm{A/cm^2}$) for the current density J and assume that $J_{\max}=10^6$ $\mathrm{A/cm^2}$. The results shown in Fig. 2 have been obtained for the following values of the parameters of the QDIP system: $E_t=30\epsilon$ and $E_J/J=0.1\epsilon/(\mathrm{A/cm^2})$. We can see from the figure that in all cases, the photocurrent through the system of small quantum dots ($\alpha=1$) is larger than that through the system of large quantum dots ($\alpha=0$). This fact also illustrates the advantage of quantum dot over quantum well IPs. That is, under the same conditions (bias voltage and other parameters) the quantum dot infrared photodetector becomes more sensitive to the external radiation than the quantum well infrared photodetector. This advantage is completely due to the Pauli exclusion principle.

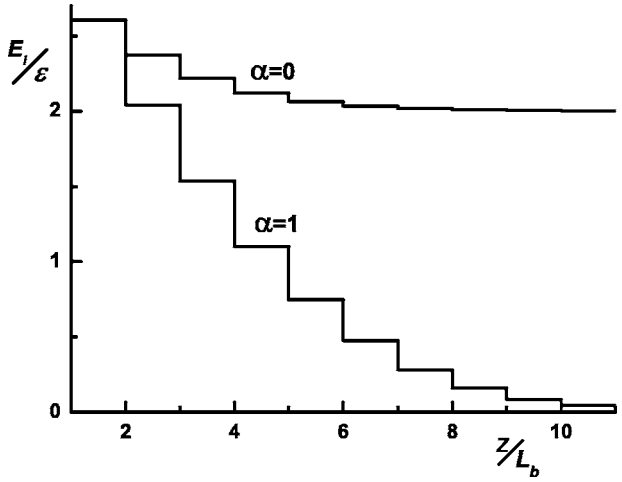

FIG. 3. Distribution of the electric field along QDIP with $N=10$ quantum dot layers for $\alpha=0$ and $\alpha=1$.

To illustrate the fact that the current through QDIP is enhanced for the system with strong exclusion principle, $\alpha=1$, we present in Fig. 3 the distribution of electric field along QDIP for $N=10$ quantum dot layers. The distribution of the electric field is shown as a function of z coordinate oriented along the growth direction of the structure. The results for both small and large quantum dots are shown in the figure. The electric field in the first barrier and, correspondingly, the current through the system [see Eq. (12)] are the same in both cases. For small quantum dots, when the Pauli principle for electrons becomes important, i.e., $\alpha=1$, the quantum dots are less occupied than in the case of large quantum dots, i.e., $\alpha=0$. This fact results in a larger positive charge accumulation in the quantum dot layers and larger steps in the electric field dependence for the systems with $\alpha=1$ compared to the systems with $\alpha=0$. Finally, the voltage drop across QDIP, given by the area under $E(z)$ dependence, is smaller in the systems with $\alpha=1$.

Under a fixed bias voltage, the photocurrent through the system monotonically increases with increasing the intensity of photon flux, which is proportional to the generation rate g. For the system under consideration, it is easier to present this dependence by keeping the current through QDIP constant and looking at the dependence of the bias voltage on the intensity of the photon flux or on the inverse effective electric field, $1/E_J \propto g$. In Fig. 4, the typical dependence of the bias voltage on the intensity of photon flux is shown for different values of parameter α and for different numbers of quantum dot layers. The current in all cases is constant and equals to $J=100$ $\mathrm{A/cm^2}$. All other parameters are the same as in Fig. 2, i.e., $J_{\max}=10^6$ $\mathrm{A/cm^2}$ and $E_t=30\epsilon$. Similar to the results of Fig. 2, the system with $\alpha=1$, i.e., with the Pauli exclusion principle, requires a smaller voltage than the system with $\alpha=0$, although the difference between the voltages, i.e., the difference between the systems with different α, is suppressed with increasing the intensity of the photon flux. This effect can be easily understood from Eqs. (1) and (2). The exclusion principle affects the rate of relaxation through

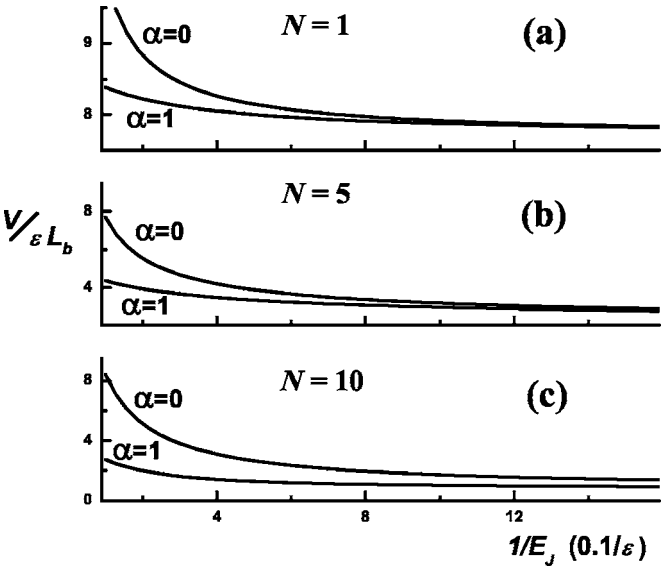

FIG. 4. Bias voltage is shown as a function of inverse effective electric field at fixed value of photocurrent, $J=100$ A/cm^2. The inverse effective electric field is proportional to photon flux. The values of α are shown. The numbers of quantum dot layers are (a) $N=1$, (b) $N=5$, and (c) $N=10$.

the number of available states in the quantum dots $(1-\alpha f_i)$. With increasing the intensity of photon flux, the electron occupation of the dots and correspondingly the product αf_i decrease,[18] which suppresses the effect of the Pauli exclusion principle.

B. Low-frequency noise

The noise of photocurrent and dark current in QWIP has been the subject of both experimental and theoretical studies in the last decade.[19–26] Different aspects of current noise have been discussed within noncorrelating electron system. Here, we address the effects of the Fermi-Dirac statistics of electrons on the current noise in QDIP. We calculate the spectrum of the current noise following the standard procedure of solution of stochastic Langevin equation[27,28] with Poisson sources of generation-recombination noise $\Delta_i^{(\mathrm{gr})}$. Since the noise results in just small corrections to a steady solution of the problem, we apply the perturbation approach to find the current noise in the system. The fist step in this approach is to search the solution of the problem as the sum of steady solution (without noise sources) and the small fluctuating parts, which finally will be proportional to the noise sources. We replace the electron concentration by $n_i+\delta n_i(t)$, the electron occupation of the quantum dot layers by $f_i+\delta f_i(t)$, and the electric field in the barriers by $E_i+\delta E_i(t)$, where n_i, f_i, and E_i stand for the steady solutions. In general, the noise sources $\Delta_i^{(\mathrm{gr})}(t)$ and correspondingly the fluctuations $\delta n_i(t)$, $\delta f_i(t)$, and $\delta E_i(t)$ depend on time. Below, we study only the case of low-frequency noise and solve the system of equations (1)–(8) in the low-frequency limit. Then, time derivatives, which are proportional to the frequency, are small and can be replaced by zeros in Eqs. (1) and (2). We also assume that the bias voltage is fixed, so the fluctuations of the voltage are zero. Finally, we obtain the nonlinear system of equations with respect to fluctuations, which should be transformed within the perturbation approach into a linear system of equations. We express the fluctuations of electron concentrations and electron occupations in terms of fluctuations of electric field and finally obtain the system of equations for fluctuations of the electric fields in the barriers. The system has the following form:

$$\delta E_{i+1} = \psi_i \delta E_i + \phi_i \delta E_1 - \eta_i \Delta_i^{(\mathrm{gr})}, \tag{15}$$

$$\sum_{i=1}^{N+1} \delta E_i = 0, \tag{16}$$

where the second equation [Eq. (16)] is the condition that the bias voltage is fixed. The coefficients ψ_i, ϕ_i, and η_i do not depend on the fluctuations and can be expressed through the stationary solution of the problem as follows:

$$\psi_i = 1 - \frac{\epsilon E_J}{(E_i + \alpha E_J)^2}, \tag{17}$$

$$\phi_i = \left(\frac{\epsilon E_t}{E_1^2}\right) \frac{E_i E_J}{(E_i + \alpha E_J)^2}, \tag{18}$$

$$\eta_i = \left(\frac{\epsilon}{g N_D}\right) \frac{E_i}{E_i + \alpha E_J}. \tag{19}$$

The solution of the linear system of equations (15) and (16) can be written as

$$\delta E_1 = \frac{\sum_{i=1}^{N} \eta_i \Delta_i^{(\mathrm{gr})} \sum_{n=i}^{N} \Psi_{i+1}^n}{1 + \sum_{n=1}^{N} \left(\Psi_1^n + \sum_{i=1}^{n} \phi_i \Psi_{i+1}^n \right)}, \tag{20}$$

$$\delta E_{n+1} = \delta E_1 \left(\Psi_1^n + \sum_{i=1}^{n} \phi_i \Psi_{i+1}^n \right) - \sum_{i=1}^{n} \eta_i \Delta_i^{(\mathrm{gr})} \Psi_{i+1}^n, \tag{21}$$

$$n = 1, \ldots, N,$$

where the following notations have been introduced:

$$\Psi_i^n = \begin{cases} 1 & \text{if } i > n \\ \prod_{j=i}^{n} \psi_j & \text{if } i \leq n. \end{cases} \tag{22}$$

The next step is to find the expression for the fluctuating part of the total current through QDIP system. It follows from Eqs. (15) and (16) that, similar to the stationary case, in the low-frequency limit the fluctuating part of the current remains the same along QDIP. Then, the fluctuations of the current density are determined by the fluctuations of the electric field in the first barrier and are given by the expression

$$\frac{\delta J}{J} = \frac{E_t \delta E_1}{E_1^2}. \tag{23}$$

Since $\Delta_i^{(\mathrm{gr})}$ is a Poissonian process with power spectral density $4gf_iN_D$, we can easily find from Eqs. (20) and (23) the power spectral density of current density fluctuations, $S_J \propto \langle \delta J \delta J \rangle$. It is given by the expression

$$S_J = \frac{4J^2}{g}\left(\frac{E_J E_t^2}{E_1^4}\right)\frac{\sum_{i=1}^{N}\frac{1}{E_i+\alpha E_J}\left(\sum_{n=i}^{N}\eta_i\Psi_{i+1}^n\right)^2}{\left[1+\sum_{n=1}^{N}\left(\Psi_1^n+\sum_{i=1}^{n}\phi_i\Psi_{i+1}^n\right)\right]^2}. \tag{24}$$

Expression (24) is valid for any number of quantum dot layers. To understand the dependence of the current noise on parameter α, we analyze, at first, the case of a single layer of quantum dots, $N=1$. Substituting $N=1$ into Eq. (24), we obtain the expression for the spectrum of the current noise of QDIP with one active layer:

$$S_J = \frac{4J^2}{g}\left[\frac{E_J E_t^2}{E_1^4(E_1+\alpha E_J)}\right]\left(\frac{\eta_1}{1+\psi_1+\phi_1}\right)^2. \tag{25}$$

It is convenient to introduce the ratio $S_J(\alpha=1)/S_J(\alpha=0)$, which characterizes suppression or enhancement of the current noise due to the Pauli principle. This ratio can be written as

$$F(x,y) = \frac{S_J(\alpha=1)}{S_J(\alpha=0)} = \frac{x(x+1)(x+y)^2}{[x^2+x(2+y)+1]^2}, \tag{26}$$

where we have used Eqs. (17)–(19) and introduced two dimensionless variables,

$$x = \frac{2E_1^3}{\epsilon E_t E_J}, \tag{27}$$

$$y = \frac{\epsilon E_t}{2E_1^2}. \tag{28}$$

The ratio $F(x,y)$ monotonically decreases as a function of y at a fixed value of parameter x, and it has nontrivial dependence on x at a fixed value of y. This dependence is shown in Fig. 5(a). At small fixed values of y, the function $F(x)$ monotonically increases, remaining smaller than 1 at all x. At larger values of y, the function $F(x)$ has a maximum, and within some interval of x it becomes larger than 1. Finally, we can summarize the dependence of $F(x,y)$ on parameters x and y by showing the domains of $F>1$ and $F<1$ in the (x,y) plane, see Fig. 5(b). The solution of equation $F(x,y)=1$ gives the boundary between the regions $F>1$ and $F<1$. This solution is given by the expression

$$y_b(x) = 1 + x + (1+2x)\left(\frac{1+x}{x}\right)^{1/2}, \tag{29}$$

and is shown in Fig. 5(b) by the solid line. The function $y_b(x)$ has a minimum at $x=x_{\min}\approx 0.245$, where $y_b(x_{\min})\approx 4.6$.

We can see from Eqs. (7), (27), and (28) that both variables x and y depend on the current and, correspondingly, on the bias voltage. When we change the current through the QDIP, we change both x and y. It is easy to find the relation between x and y, which does not depend on the bias voltage and electric current. From Eq. (28), we find the electric field in the first barrier E_1 in terms of parameter y. Note that electric field E_1 is completely determined by electric current J through QDIP, see Eq. (7). Then, we substitute $E_1(y)$ into Eq. (27). Here, we should also take into account the dependence of E_J on the current density. Finally, we obtain the relation between x and y,

$$x = \frac{\mu g}{sJ_{\max}}\left(\frac{\epsilon E_t}{2}\right)^{1/2}\frac{\exp\left(\sqrt{\frac{2E_t y}{\epsilon}}\right)}{y^{3/2}}, \tag{30}$$

which describes the line in the (x,y) plane and characterizes the property of a given system of QDIP. The typical line [Eq. (30)] is shown in Fig. 5(b) by the dotted line. Taking into account that parameter y decreases with increasing the current through QDIP [see Eq. (28)], we can conclude that when the current density through QDIP increases, then the (x,y) point is moving along the line [Eq. (30)] from larger to lower values of y. Therefore, when we increase the current density, the system goes from region $F>1$ to region $F<1$. At lower currents through the QDIP system, the current noise is enhanced by the Pauli exclusion principle, while at large currents the current noise is suppressed.

This tendency remains the same for a larger number of quantum dot layers. Using the same parameters for QDIP as in Fig. 2, i.e., $J_{\max}=10^6$ A/cm^2, $E_t=30\epsilon$, and $E_J/J=0.1\epsilon/(\mathrm{A/cm^2})$, we calculate the low-frequency power spec-

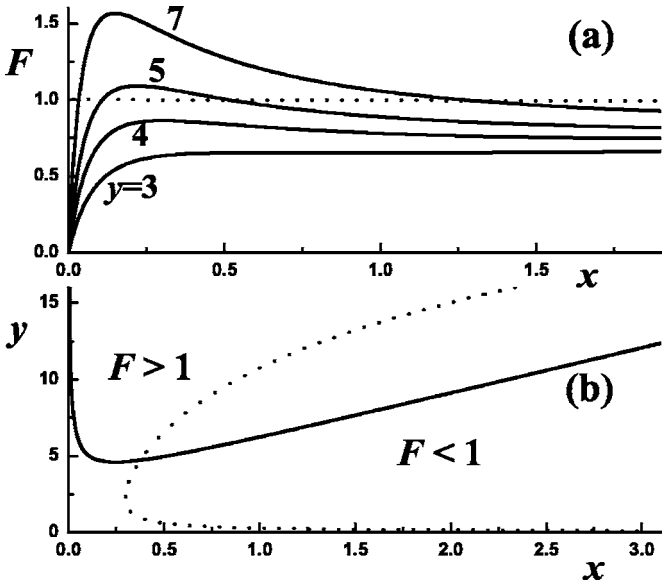

FIG. 5. (a) The function $F(x,y)$ given by Eq. (26) is shown for different values of y. The numbers by the lines are the values of y. The dotted line corresponds to $F=1$. (b) Regions $F(x,y)>1$ and $F(x,y)<1$ are shown in the (x,y) plane. The solid line is the boundary between the regions. The solid line is described by Eq. (29). The dotted line corresponds to a given QDIP. The current through QDIP is changed along the dotted line.

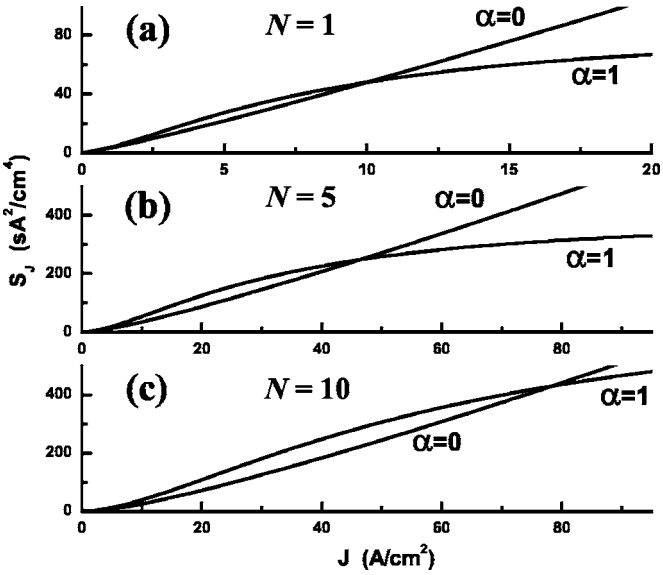

FIG. 6. Low-frequency spectral density of current noise is shown as a function of current density for different numbers of quantum dot layers: (a) $N=1$, (b) $N=5$, and (c) $N=10$.

tral density of the current noise S_J for different numbers of quantum dot layers N. The results of the calculations are shown in Fig. 6. We can see that in all cases, the current noise is enhanced for $\alpha=1$ compared to $\alpha=0$ when the current is small enough. At larger values of the current, the current noise in suppressed for $\alpha=1$ compared to $\alpha=0$. We can also see from Fig. 6 that the crossover point between these two regimes moves to higher currents when the number of quantum dot layers increases.

IV. DISCUSSION

The system of equations (1)–(3) describes two main processes which determine the properties of the present model of QDIP: (i) the first one is the generation-recombination process [Eq. (2)], which introduces the relation between the electron density in the ith barrier and the population of the ith quantum dot layer, and (ii) the second process is the screening of the electric field by the electrons in the quantum dot layer [Eq. (3)], which determines the relation between the electric field in the $(i+1)$th and ith barriers in terms of the electron occupation of the ith quantum dot layer. Based on these equations, we can make some conclusions about the effects of the Pauli exclusion principle on the I-V structure of the QDIP.

In the steady regime without the noise source, we can see that the equilibrium populations of the quantum dots are proportional to $f_i \propto (1+\alpha)^{-1}$. This means that in the system with the Pauli principle; i.e., in the QDIP system, the electron concentration in the quantum dot layer is less than that in the system without Pauli principle, i.e., in the QWIP. This dependence can also be understood from the fact that with the Pauli principle, the relaxation current becomes suppressed since it is proportional to the number of available states in the dot system (Pauli principle). In the steady condition, the relaxation current should be equal to the generation current. Then, suppression of relaxation current means that more electrons can be generated from the quantum dot layer; i.e., the population of the quantum dot layer is less in the system with the Pauli principle. Since initially the quantum dot layer is neutral, the smaller electron population means that the larger (positive) charge is accumulated in the quantum dot layer. The larger electric charge of the layer introduces the higher steps of the electric field across the dot layer, or the larger screening of the electric field by the charge in the layer (see Fig. 3). If we start from the same electric field in the first barrier, i.e., at the same current through the photodetector, then, since the voltage drop across the infrared photodetector is proportional to the electric field in each barrier region, the voltage drop across the QDIP (with Pauli principle) is smaller than the voltage drop across the QWIP (without Pauli principle). This dependence is illustrated in Fig. 2. Therefore, for a given number of active layers and a given value of the current through infrared photodetector, the voltage drop across QDIP will be less than the voltage drop across QWIP.

The analysis of the noise in the QDIP and QWIP is more complicated since it is determined by competitions of different factors. If we consider just generation and recombination processes, then the noise of the generation-recombination current will be suppressed in the system with the Pauli principle. This is because the Pauli principle introduces an additional correlation[6] in the recombination process; i.e., if this is an electron in the quantum dot, then the relaxation of another electron from the continuum to this quantum dot is prohibited. Therefore, the noise becomes suppressed if we take into account the Pauli principle. In the photodetector system, the current through the system is determined not only by the generation-recombination processes but also by the screening of the electric field along the photodetector. This introduces a more complicated dependence of the current noise on the strength of the Pauli principle, α.

To understand the origin of this dependence we, at first, analyze the fluctuations of the electric field in different barriers. As we can see from Eq. (3), the fluctuations of the electric field in the $(i+1)$th barrier are determined by the fluctuations of the electric field in the ith barrier and by the fluctuation of the occupation of the ith quantum dot layer, δf_i. The fluctuations of the occupation of the dot layer depend on the generation-recombination source noise in the ith layer and on the fluctuation of the electron density in the ith barrier, δn_i. Due to conservation of the current, the fluctuation δn_i is determined by the fluctuations of the electric field in the ith barrier and by the fluctuation of the current (or fluctuation of the electric field in the first barrier). Therefore, the fluctuation δf_i depends on the fluctuations of the electric field in the ith and in the first barriers. Finally, we can see from Eq. (15) that the fluctuations of the electric field in the $(i+1)$th barrier are determined by the fluctuations of the electric field in the ith barrier with the coefficient ψ_i and by the fluctuations of the electric field in the first barrier with the coefficient ϕ_i. There is also a dependence on the noise source Δ_i. The coefficient η_i next to the noise source decreases with increasing parameter α. This decrease is due to correlations induced by the Pauli principle in the recombination rate. The coefficient η_i contributes to the suppression of the noise in

the QDIP. The coefficients ψ_i and ϕ_i have opposite dependences on the parameter α: the coefficient ψ_i increases while the coefficient ϕ_i decreases with increasing α. Therefore, the fluctuations of the electric field in the $(i+1)$th barrier are determined by two tendencies with increasing parameter α: the first one is enhancement of fluctuation due to factor ϕ_i, and the second one is suppression of fluctuations due to factor ψ_i. Since ψ_i is inversely proportional to the electric field, the suppression of fluctuations is more pronounced at smaller electric field, i.e., at smaller values of the current. Therefore, in the units of the fluctuations of the electric field in the first barrier, the fluctuations of the electric field in the $(i+1)$th barrier decrease with increasing α at small values of the current and increase with α at large values of the current. Since the voltage drop across the photodetector is fixed, i.e., the sum of the fluctuations of the electric field in all barriers is zero, the above tendency means that at small values of the current the fluctuations of the electric field in the first barrier, i.e., the fluctuations of the current [see Eq. (11)], are enhanced at small and suppressed at large values of the current in the QDIP compared to QWIP. This behavior is illustrated in Fig. 6.

With increasing the number of the active regions of the photodetectors, the coefficients ψ_i become effectively enhanced [see Eq. (20)] by additional factors, which results in the wider region within which the current noise in QDIP is enhanced compared to QWIP (Fig. 6).

V. CONCLUSION

In the present paper, we have studied the effects of the Pauli exclusion principle on the properties of quantum dot infrared photodetectors. In the model discussed above, we assumed that the exclusion principle is characterized by a single constant, α, which can take values from 0 (for the systems without the Pauli principle) to 1 (for the systems with the Pauli principle). In the above analysis, we discussed only the effect of parameter α on the characteristics of QDIP and kept all other parameters of the systems constant. The main conclusion of the present research is that the Pauli exclusion principle makes the system more sensitive to the external illumination; i.e., under the same bias voltage, the photocurrent is the largest in the systems with the exclusion principle. In terms of the type of infrared photodetectors, this statement means that QDIP is more sensitive to external illumination than QWIP. The advantage of QDIP over QWIP has already been discussed in the literature,[5] where the values of photogeneration and relaxation rates in QDIP were compared to those in QWIP.

Another advantage of QDIP over QWIP is suppression of low-frequency photocurrent noise at high bias voltage. This suppression is due to the Pauli principle, which has already been discussed for the system of quantum dots.[6] The specific feature of the QDIP is that at low bias voltage, the tendency is opposite and the current noise in QDIP is enhanced compared to that in QWIP.

The main processes which have been taken into account in the above analysis are bound to continuum transitions due to photoabsorption and continuum to bound transitions due to relaxation. In this case, the electronic system can be approximately described as the combination of two systems: the system of electrons in the bound states of quantum dots and the system of electrons in the continuum states. Transitions between these two systems determine the properties of infrared photodetectors. For different types of photodetectors, the generation of photocurrent can be a more complicated process. For example, for bound to bound transitions, the electrons are photoexcited into bound excited states of the system and then by tunneling or by thermal excitation transport into continuum states. In this case, the rate equations should take into account the population of the excited bound states of the active regions of photodetectors.

In the above analysis, we assumed also that electrons are spinless particles and each level of the dot can be occupied only by a single electron. The spin degrees of freedom make each level double degenerate. For weak interelectron interaction, this degeneracy can be incorporated into the above model by increasing the density N_D of electrons in the dot layer by a factor of 2. For small quantum dots, interelectron interactions can be strong. In this case, if the electron density is small enough, then each dot will be occupied by less than one electron and the approach will be the same as for the spinless particles. For larger electron density, the interaction effects become important and more detailed analysis should be done. The interactions can modify not only the strength of the response of photodetectors but also the shape of the absorption line.[29]

[1] B. F. Levine, J. Appl. Phys. **74**, R1 (1993).
[2] V. Ryzhii, Semicond. Sci. Technol. **11**, 759 (1996).
[3] D. Pan, E. Towe, and S. Kennerly, Appl. Phys. Lett. **73**, 1937 (1998).
[4] S. Krishna, S. Raghavan, G. von Winckel, A. Stintz, G. Ariyawansa, S. G. Matsik, and A. G. U. Perera, Appl. Phys. Lett. **83**, 2745 (2003).
[5] V. Ryzhii, I. Khmyrova, M. Ryzhii, and V. Mitin, Semicond. Sci. Technol. **49**, 8 (2004).
[6] L. Y. Chen and C. S. Ting, Phys. Rev. B **43**, 4534 (1991).
[7] L. P. Kouwenhoven, C. M. Marcus, P. McEuen, S. Tarucha, R. Westervelt, and N. S. Wingreen, in *Mesoscopic Electron Transport*, edited by L. L. Sohn, L. Kouwenhoven, and G. Schon, NATO Advanced Studies Institute, Series E: Applied Science, Vol. 345 (Kluwer, Dordrecht, 1997).
[8] J. Urayama, T. B. Norris, J. Singh, and P. Bhattacharya, Phys. Rev. Lett. **86**, 4930 (2001).
[9] M. Ershov, V. Ryzhii, and C. Hamaguchi, Appl. Phys. Lett. **67**, 3147 (1995).
[10] F. E. Zocchi, Phys. Rev. B **73**, 035203 (2006).
[11] M. Ryzhii and V. Ryzhii, Jpn. J. Appl. Phys., Part 1 **38**, 5922 (1999).

[12] M. Ryzhii, V. Ryzhii, and M. Willander, Jpn. J. Appl. Phys., Part 1 **38**, 6650 (1999).
[13] V. Ryzhii and R. Suris, Jpn. J. Appl. Phys., Part 1 **40**, 513 (2001).
[14] V. Ryzhii, I. Khmyrova, M. Ryzhii, R. Suris, and C. Hamaguchi, Phys. Rev. B **62**, 7268 (2000).
[15] C. M. Van Vliet, IEEE Trans. Electron Devices **41**, 1902 (1994).
[16] V. Ryzhii, J. Appl. Phys. **81**, 6442 (1997).
[17] V. Ryzhii, M. Ryzhii, and H. C. Liu, J. Appl. Phys. **92**, 207 (2002).
[18] V. Ryzhii, Jpn. J. Appl. Phys., Part 2 **40**, L148 (2001).
[19] H. C. Liu, Appl. Phys. Lett. **61**, 2703 (1992).
[20] W. A. Beck, Appl. Phys. Lett. **63**, 3589 (1993).
[21] A. Carbone and P. Mazzetti, Phys. Rev. B **49**, 7592 (1994).
[22] V. D. Shadrin, V. V. Mitin, V. A. Kochelap, and K. K. Choi, J. Appl. Phys. **77**, 1771 (1995).
[23] A. Carbone and P. Mazzetti, Appl. Phys. Lett. **70**, 28 (1997).
[24] M. Ersov and A. N. Korotkov, Appl. Phys. Lett. **71**, 1667 (1997).
[25] M. Ershov and H. C. Liu, J. Appl. Phys. **86**, 6580 (1999).
[26] A. Carbone, R. Introzzi, and H. C. Liu, Appl. Phys. Lett. **82**, 4292 (2003).
[27] P. Langevin, C. R. Hebd. Seances Acad. Sci. **146**, 530 (1908).
[28] I. Karatsas and S. Shreve, *Brownian Motion and Stochastic Calculus*, 2nd ed. (Springer-Verlag, New York, 1997).
[29] David M.-T. Kuo and Y.-C. Chang, Phys. Rev. B **67**, 035313 (2003).